

Short Communicaton

One-step Synthesis of Low-cost and High Active Li_2MnO_3 Cathode Materials

Guanrao Liu, and Shichao Zhang*

School of Materials Science & Engineering, Beijing University of Aeronautics & Astronautics, Beijing 100191, China

*E-mail: csc@buaa.edu.cn

Received: 5 April 2016 / Accepted: 11 May 2016 / Published: 4 June 2016

Nanostructured (10~50 nm) cathode material Li_2MnO_3 was simply prepared via facile one-step hydrothermal process without any further treatment by controlling reaction parameters, including the reaction time, proportion of processor, and the reagent concentration. The obtained Li_2MnO_3 products were well crystallized by a monoclinic structure with a space group of $C2/m$ phase. The materials exhibit a lower activation potential when being cycled, and delivered electrochemical performance between 4.3V and 2.0 V at room temperature, with a capacity of $243 \text{ mAh}\cdot\text{g}^{-1}$. The structural information of the prepared materials advances the understanding of corresponding electrochemical properties.

Keywords: Li_2MnO_3 , Cathode Materials, Hydrothermal, Lithium-ion Batteries.

1. INTRODUCTION

Extensive researches have shown the significant role of nano-size effect to build-up the thermodynamic and kinetic properties of lithium reactive materials. With the advantages of low cost, abundance and environmental benign, lithium manganese oxide based compounds are the most attractive cathode materials for lithium ion batteries (LIB) [1-11]. Various Mn based derivatives such as spinel-structured LiMn_2O_4 and $\text{Li}_4\text{Mn}_5\text{O}_{12}$, orthorhombic or mono-clinic structured LiMnO_2 , and other lithium-rich structures have caught the eyes of many researchers, however, LiMnO_2 tends to transform into a spinel structure because of the cation migration during the lithium insertion/extraction process [12]; LiMn_2O_4 suffers from capacity loss resulted from manganese dissolution and the Jahn–Teller effect [5, 13]. In these Li-Mn-O materials, Li_2MnO_3 component has been investigated thoroughly as the role of providing Li^+ ions and stabilizing the electrode structure. Delmas et al. [14] described that Li_2MnO_3 possesses an O_3 -type structure similar to layered LiMO_2 notation, which can

be alternatively represented as $\text{Li}[\text{Li}_{1/3}\text{Mn}_{2/3}]\text{O}_2$, i.e. 1/3 of Mn^{4+} ions in interslab octahedral sites are replaced with Li^+ ions, while slab octahedral sites were occupied by the rest of Li and Mn^{4+} ions. A lithium-rich layered superstructure with the honeycomb Li/Mn orders formed due to the occupation of additional Li^+ ions in transition metal (TM) layers, which are basically derived from the layered rock-salt $\alpha\text{-NaFeO}_2$ type structure with space group of $R\bar{3}m$. Layer-structured Li_2MnO_3 is thermodynamically stable, in which Li^+ ions are mobile and can be extracted from the structure on charging process. Therefore, Li_2MnO_3 is considered as potential cathode materials for LIB.

Li_2MnO_3 is generally considered as electrochemically “inactive” below the usual cut-off charge potential of 4.5V vs. Li/Li^+ because it is difficult to oxidize Mn^{4+} to the Mn^{5+} state [15-18]. The high charge voltage also requires further modified electrolyte, and bring in other problems such as the stability, or safety of cells. To achieve low-cost batteries with high performance, simple, inexpensive, highly reproducible and environmental friendly methods are employed for producing electrode materials, such as solid state synthesis, co-precipitation and pyrolysis [19-21]. Co-precipitation or sol-gel processes can produce many kinds of nanosized cathode materials; however, the process presents challenges in terms of extending annealing conditions because of poor crystallization, resulting in an unpredictable wide range of particle size and specific surface area, which highly influence the electrochemical performance of the materials such as capacity and rate capability. Single-crystalline Li_2MnO_3 nanorods were prepared by Wang et al. using a low-temperature molten salt synthetic route while no electrochemical performance was tested [22]. Kubota et al. [23] obtained oxygen-deficient $\text{Li}_2\text{MnO}_{3-x}$ ($0 < x < 0.19$) using metal hydrides as reducing agents at 255-265°C, which delivers a very large capacity in the 1st cycle. However, all the methods mentioned above suffered from some problem such as high energy consumption, expensive raw materials, and complex process.

Self-seeding hydrothermal methods can be employed to synthesize Li-Mn-O nanostructures. In this article, well-crystallized Li_2MnO_3 nanoparticles were obtained via one-step hydrothermal method by controlling preparation parameters, including reaction time, proportion of processor, and the reagent concentration. The prepared materials delivered a reversible capacity of 243 $\text{mAh}\cdot\text{g}^{-1}$ charged/discharged between 2.0-4.3V, which is different previously reported results.

2. EXPERIMENTAL

2.1. Preparation of Li_2MnO_3 nanoparticles

KMnO_4 and MnSO_4 with the molar ratio of 1: 4 were dissolved in distilled water. And, excess LiOH solution was added into the mixed solution. A brown suspension was immediately formed as soon as LiOH solution was added. Then, the mixtures with suspension were transferred into a Teflon-lined stainless steel autoclave for a hydrothermal reaction at 200°C for 32 h. Finally, the obtained precipitate washed thoroughly with distilled water and ethanol, and dried at 60°C in air.

2.2. Structure Characterization

X-ray powder diffraction (XRD) measurements were employed to investigate the

crystallographic structure using a Rigaku Rint2200 X-ray diffractometer with a non-monochromated Cu-K α X-ray source. The morphology and structure of prepared materials were exhibited by transmission electron microscopy (TEM) and high-resolution transmission electron microscopy (HRTEM) images recorded with a JEOL-2010 instrument at an acceleration voltage of 200 kV.

2.3. Electrochemical measurements

Electrochemical properties of the prepared samples were measured using Swagelok-type two-electrode cells. The working electrodes were pressed with a mixture of 80 wt.% active materials, 15 wt.% acetylene black, and 10 wt.% polytetrafluoroethylene (PTFE) binders. Then, the prepared electrodes were dehydrated by a vacuum dry at 60°C for 12 h and were cooled down to room temperature. The cells assembled in an MBraun glove box filled with pure argon flow. A lithium disk and a lithium chip served as counter and reference electrodes. The electrolyte was 1M LiPF₆ dissolved in ethylene carbonate (EC) and dimethyl carbonate (DMC) solution (EC:DMC=1:1, v/v). Celgard 2300 polypropylene was employed as the separator. Galvanostatic charge/discharge cycling was studied in the potential range 4.3–2V vs. Li/Li⁺ using a Newware multi-channel battery testing system.

3. RESULT AND DISCUSSION

3.1. Structures and Morphologies Analysis

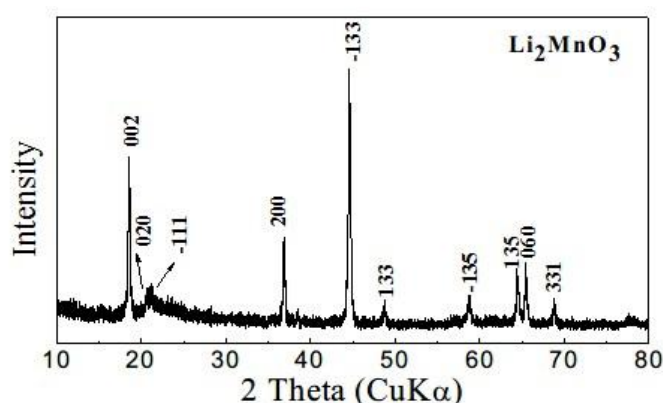


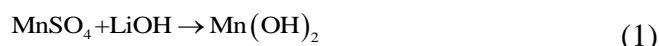
Figure 1. XRD patterns of nanostructured monoclinic Li₂MnO₃ prepared at 200°C with the precursor MnSO₄, KMnO₄, and LiOH

The phase structure of obtained products was determined by XRD measurements. As shown in Figure 1, the observed diffraction peaks of the samples match well with the Li₂MnO₃ structure, and none impurity phases were detected in the products. The well-developed diffraction peaks at $2\theta = 64.5^\circ$ and 65.5° correspond to (135) and (060) directions respectively, indicating the products possess a monoclinic structure with a space group of C2/m, which is same as layered rock-salt structure with space group of $R\bar{3}m$. The (020) and (-111) peaks located at the $2\theta = 20^\circ \sim 22.5^\circ$ range are

substantially broad, and merged into one broad peak, owing to the structural defects existed in the pack of the ordered cationic layers along the “c” axis of monoclinic structures [14, 24].

Investigation for the hydrothermal systems showed that the molar ratio of $\text{MnSO}_4/\text{KMnO}_4$ and the concentration of LiOH were two key factors influencing the phase and structures of final product.

Mn^{2+} in MnSO_4 can be oxidized by KMnO_4 inevitably, which means the proportion of $\text{MnSO}_4/\text{KMnO}_4$ was essential in decision of the valence of Mn in production. By adding LiOH into the mixed solution of MnSO_4 and KMnO_4 , a precipitate of $\text{Mn}(\text{OH})_2$ was formed immediately. The precursor KMnO_4 was employed to oxidize $\text{Mn}(\text{OH})_2$, and the reaction process before lithiation is as follows:



The oxidizability of KMnO_4 was significantly impacted by the pH value of the solution. In this process, LiOH played the role of adjusting the pH value of the mixture, and also was the sources of lithium ion for preparing orthorhombic Li-Mn-O compounds. With the concentration of LiOH decreasing, Mn^{3+} was further oxidized to the value of +4, and Li_2MnO_3 phase was formed. It can be summarized as:

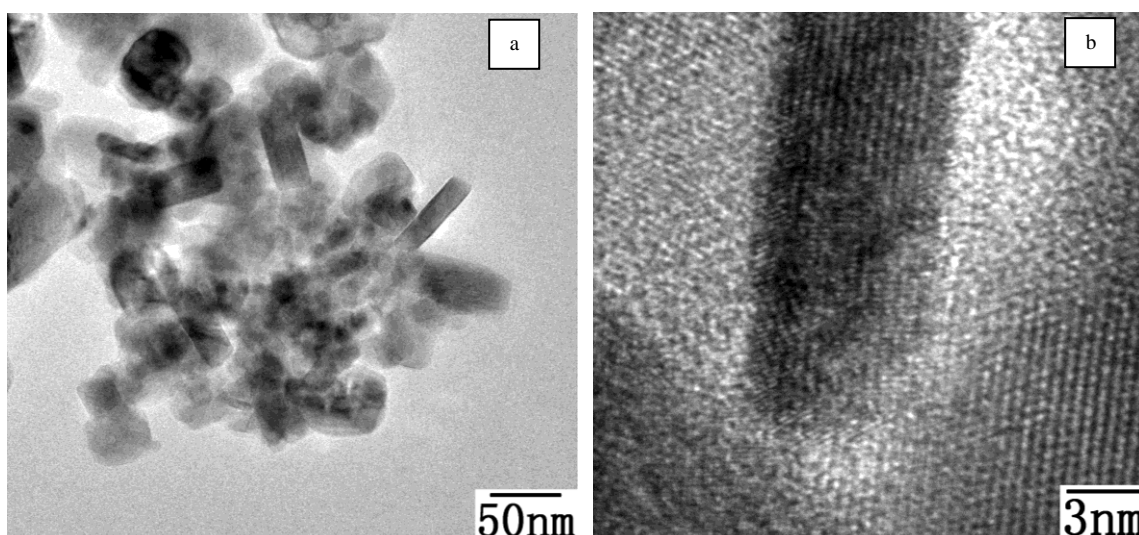
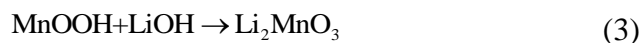


Figure 2. TEM and HRTEM images of the as-prepared Li_2MnO_3 powders

The crystallinity and morphology of the particles have great influence on the electrochemical performance of electrode materials. The structures information of prepared Li_2MnO_3 powders was further investigated via TEM and HRTEM. As shown in Fig.2, the samples are agglomerated secondary particles, in other words, these particles are shaped from much smaller primary particles. The materials present a quasi-porous structure, owing to the interstices and pores between the primary particles. The final product morphology is the mixture of nanorods and nanocubes with the size of 10 ~ 50nm. The

HRTEM result implies a well crystallized status of the products, which is beneficial to the transport of Li^+ ions and the cycling stability of cathode materials, as well as the particle size of the product.

3.2. Electrochemical Properties

The electrochemical performance of the as-prepared Li_2MnO_3 nanoparticles was evaluated at by determining the charge-discharge characteristics using Swagelok-type two-electrode cells at room temperature. It can be seen from Fig.3, a specific discharge capacity of $243 \text{ mAh}\cdot\text{g}^{-1}$ was delivered between 4.3 and 2.0V. The initial discharge capacity of the product was $323 \text{ mAh}\cdot\text{g}^{-1}$, which corresponds to 70% of the theoretical capacity of Li_2MnO_3 ($459 \text{ mAh}\cdot\text{g}^{-1}$) when all the lithium ions are extracted. According to previous report [27-30], Li_2MnO_3 will be changed to MnO_2 when being charged, owing to the complete Li_2O removal from the rocksalt structure. Whereas it is probably only one lithium ion is reinserted before the formation of stoichiometric rocksalt LiMnO_2 during discharge. Therefore, the coulombically efficient of Li_2MnO_3 electrodes in first charge/discharge process is about 75%. Moreover, the efficient increased to 85% with cycling after 20cycles.

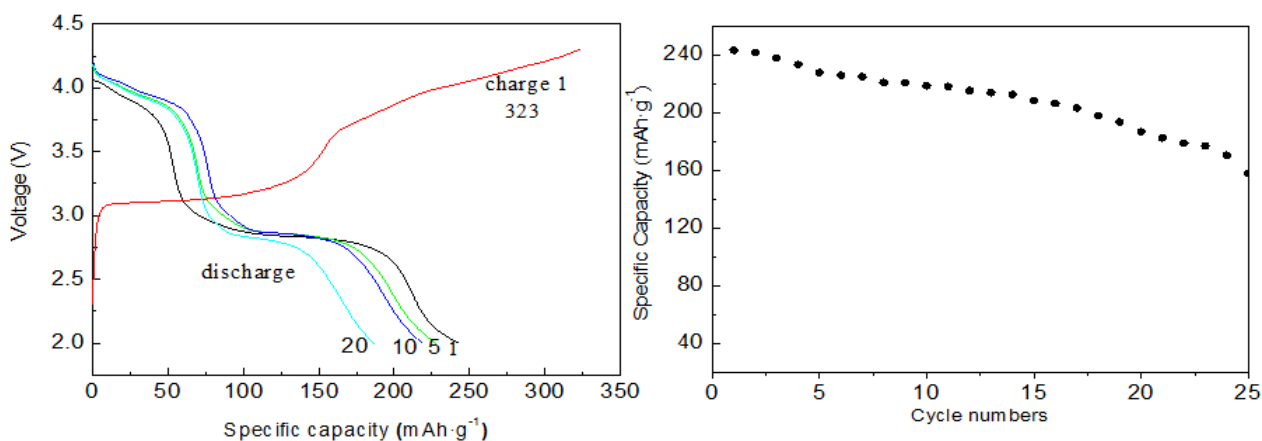


Figure 3. Cycling performance of prepared Li_2MnO_3 tested at current density of $60\text{mA}\cdot\text{g}^{-1}$ between 4.3V and 2.0 V

Usually, it is considered that the monoclinic structured Li_2MnO_3 is electrochemically “inactive” for lithium intercalation and de-intercalation between 2.0 V and 4.5 V vs Li/Li^+ . [16, 25-28], and the capacity of Li_2MnO_3 is only $20 \text{ mAh}\cdot\text{g}^{-1}$ at 4.5 V. A reasonable explanation based on oxygen loss has been accepted [28, 29]. When Li_2MnO_3 electrodes are charged above 4.5 V in the first cycle, there are two combined processes happened, corresponding to lithium de-intercalation (electrochemical process) and oxygen loss (chemical process) respectively. During these processes, Li_2O will be extracted from the Li_2MnO_3 component before electrolyte oxidation, thus Li_2MnO_3 can be electrochemically activated. In our test, a clearly lower activation potential in the initial charging was detected, which may be attributed to the vicinity of the surface, and the shallow reaction depth [30] ($<50 \text{ nm}$) of nanosized Li_2MnO_3 . Compared to bulk materials, nano-scaled particles with higher specific surface and more defects expose more Li_2MnO_3 to the electrolyte and exhibit higher energies, which can decrease the

potential barrier and make it easier for Li_2O extraction from the Li_2MnO_3 component. Moreover, the diffusion distance of Li^+ and electrons were shortened during the electrochemical process. Therefore, the surface electrochemical reactivity between electrolyte and the prepared active materials was greatly improved.

4. CONCLUSIONS

Nanostructured Li_2MnO_3 cathode material was successfully obtained via a low-cost one-step hydrothermal reaction using $\text{MnSO}_4 \cdot \text{H}_2\text{O}$, KMnO_4 and LiOH aqueous solution as the precursor at a low temperature. The cathode materials was tested between general 4.3 and 2.0V voltage window, and shows good electrochemical properties in rechargeable lithium batteries with a discharge capacity of 242 $\text{mAh} \cdot \text{g}^{-1}$. The materials exhibit a lower activation potential due to the nanoscale effect, which makes it easier for Li^+ diffusion, indicating the promising future of nanoscaled cathode materials for application in lithium ion batteries.

ACKNOWLEDGEMENT

This work was supported by the National Basic Research Program of China (973 Program) (2013CB934001), National Natural Science Foundation of China (51274017), National 863 Program of China (2013AA050904), International S&T Cooperation Program of China (2012DFR60530).

References

1. R. J. Gummow, A. de Kock, and M.M. Thackeray, *Sol. Stat. Ionics*, 69 (1994) 59.
2. P.G. Bruce, A.R. Armstrong, and R. Gitzendanner, *J. Mater. Chem.*, 9 (1999) 193.
3. M.M. Thackeray, C.S. Johnson, J.T. Vaughey, N. Li, and S.A. Hackney, *J. Mater. Chem.*, 15(2005) 2257.
4. J. Awaka, J. Akimoto, H. Hayakawa, Y. Takahashi, N. Kijima, M. Tabuchi, H. Sakaebe, and K. Tatsumi, *J. Power Sources*, 174 (2007) 1218.
5. L. He, S. C. Zhang, X. Wei, Z. J. Du, G. R. Liu, and Y. L. Xing, *J. Power Sources*, 220 (2012) 228
6. H. Yu, H. Zhou, *J. Phys. Chem. Lett.*, 4(2013)1268.
7. S. J. Kim, Y. W. Lee, B. M. Hwang, S. B. Kim, W. S. Kim, G. Z. Cao, and K. W. Park, *RSC Adv.*, 4(2014)11598
8. P. F. Yan, L. Xiao, J. M. Zheng, Y. G. Zhou, Y. He, X. T. Zu, S. X. Mao, J. Xiao, F. Gao, J. G. Zhang, and C. M. Wang, *Chem. Mater.*, 27(2015) 975
9. F. Dogan, J. R. Croy, M. Balasubramanian, M. D. Slater, H. Iddir, C. S. Johnson, J. T. Vaughey, and B. Key, *J. Electrochem. Soc.*, 162(2015) A235
10. D. Kim, J. M. Lim, Y. G. Lim, M. S. Park, Y. J. Kim, M. Cho, and K. Cho, *ChemSusChem*, 8(2015) 3255
11. D. Wang, X. Y. Wang, R. Z. Yu, Y. S. Bai, G. Wang, M. H. Liu, and X. K. Yang, *Electrochim. Acta*, 190(2016)1142
12. B. Ammundsen, J. Paulsen. *Adv. Mater.*, 13 (2001) 943
13. L. L. Xiong, Y. L. Xu, T. Tao, J. Song, J. B. Goodenough, *J. Mater. Chem.*, 22(2012)24563
14. A. Boulineau, L. Croguennec, C. Delmas, and F. Weill, *Chem. Mater.*, 21 (2009) 4216
15. M. M. Thackeray, *Progress Sol. Stat. Ionics*, 25(1997) 1.
16. A.R. Armstrong, A.D. Robertson, and P.G. Bruce, *J. Power Sources*, 146 (2005)275.

17. S. F. Amalraj, L. Burlaka, C. M. Julien, A. Mauger, D. Kovacheva, M. Talianker, B. Markovsky, and D. Aurbach, *Electrochim. Acta*, 123 (2014) 395
18. Y. Nakao, K. Ozawa, Y. Nemoto, F. Uesugi, H. Fujii and T. Mochiku, *J. Ceram. Soc. Jap.*, 123(2015)589
19. L. Xiao, J. Xiao, X. Q. Yu, P. F. Yan, J. M. Zheng, M. Engelhard, P. Bhattacharya, C. M. Wang, X. Q. Yang, and J. Guang Zhang, *Nano Energ.*, 16 (2015) 143
20. L. Xue, S. Zhang, S. Li, Y. Lu, O. Toprakci, X. Xia, C. Chen, Y. Hu, and X. Zhang, *J. Alloy Compd.*, 577(2013)560
21. Q. Zhang, X. Hu, D. Zhan, and T. Peng, *Electrochim. Acta*, 113(2013)424.
22. X. Wang, J.M. Song, L.S. Gao, H.G. Zheng, M.R. Ji, and Z.D. Zhang, *Sol. Stat. Commun.*, 132 (2004)783.
23. K. Kubota, T. Kaneko, M. Hirayama, M. Yonemura, Y. Imanari, K. Nakane, and R. Kanno, *J. Power Sources*, 216 (2012)249.
24. J. Breger, M. Jiang, N. Dupre, Y.S. Meng, Y. Shao-Horn, G. Ceder, and C.P. Grey, *J. Sol. Stat. Chem.*, 178 (2005) 2575.
25. C. S. Johnson, J. S. Kim, C. Lefief, N. Li, J. T. Vaughey, and M. M. Thackeray, *Electrochem. Commun.*, 6(2004) 1085
26. M. Kundu, C. C. A. Ng, D. Y. Petrovykh and L. Liu, *Chem. Commun.*, 49(2013)8459
27. J. M. Lim, D. Kim, Y. G. Lim, M. S. Park, Y. J. Kim, M. Cho, and K. Cho, *J. Mater. Chem. A*, 3(2015)7066
28. J. S. Kim, C. S. Johnson, J. T. Vaughey, M. M. Thackeray, S. A. Hackney, W. Yoon, and C. P. Grey, *Chem. Mater.*, 16 (2004) 1996
29. Z. Lu, J.R. Dahn, *J. Electrochem. Soc.*, 149(2002) 815.
30. M. Tabuchi, Y. Nabeshima. *J. Power Sources*, 174(2007) 554.